Synthesis and Crystal Structure of $Ae_2LiInGe_2$ (Ae = Ca, Sr): New Zintl Phases with a Layered Silicate-like Network

Jiang-Gao Mao, Zhihong Xu, and Arnold M. Guloy*

Department of Chemistry and Texas Center for Superconductivity, University of Houston, Houston, Texas 77204-5641

Received April 12, 2001

Two new Zintl phases $Ae_2LiInGe_2$ (Ae = Ca **1**; Sr **2**) were obtained from stoichiometric reactions of the pure elements in sealed Nb tubing at 1000−1050 °C. The isomorphous polar intermetallic phases crystallize in the orthorhombic space group *Pnma*, with cell constants of $a = 7.2512(7)$, $b = 4.4380(5)$, and $c = 16.902(1)$ Å for compound **1**, and $a = 7.5033(8)$, $b = 4.6194(5)$, and $c = 17.473(2)$ Å for compound **2**. The crystal structure can be derived from the vertex-sharing of $InGe_{4/2}$ tetrahedral units that form "corrugated" sheets normal to the crystallographic *c*-axis. Calcium and lithium atoms act as "spacers" that effectively separate the anionic $[InGe_2]^{5-}$ layers. The layered anionic substructure is similar to those exhibited by layered metal oxides, sulfides, and silicates. The connectivity of the tetrahedral building unit, $[InGe_{4/2}]^{5-}$, is analogous and isoelectronic to the silicate $[SiO_{4/2}]$ unit.

Introduction

The Zintl concept provides a simple and useful way to rationalize relationships between stoichiometry, crystal structure, and chemical bonding in a variety of main group intermetallics.[1] In this scheme, electropositive metals act merely as electron donors, donating electrons to their more electronegative partners. The latter elements then form bonds to satisfy their octets, yielding anionic clusters, chains, layers, and networks. The application of the concept in rationalizing crystal structure−stoichiometry−property of tetrelides and pnictides, with a vast variety of anionic structures, has been quite successful. As a consequence, the concept has been widely used in directing and rationalizing the syntheses of many posttransition intermetallics.

The continuing evolution of the concept has led to explanations of nonstoichiometry, multicenter bonding and metal−metal bonding found in Zintl phases. Moreover, the assumption of the polar nature of Zintl phases has been validated by numerous theoretical and physical studies on Zintl and related polar intermetallic phases.[1−3] Hence, the efficacy and chemical simplicity of the Zintl concept describes a smooth transition from molecular bonding schemes to extended solid-state structures. It further allows for the use of simple isoelectronic and electron-counting schemes in the bonding picture of complex intermetallics.

In recent years, research on complex polar intermetallics containing Group 13 posttransition elements have focused on novel Ga, In, and Tl cluster compounds.[4,5] Chemical bonding in these "electron-deficient" systems can be rationalized in terms of the usual Wade's rules as in the boranes, and most studies on trielides have been spurred by the novelty of their cluster chemistry. Later reports on polar intermetallic trielides with mixed In−Ge anions have resulted in intriguing questions about the ability of In to accommodate high negative charges, open-shell electronic structures, and multiple bonding schemes.[1,4,6] These studies revealed the unusual electronic behavior of Zintl phases containing both Group 13 and 14 posttransition metals. Our recent studies on mixed trelide−tetrelide polar intermetallics have focused on understanding the structural, chemical, and electronic characteristics of "electron-deficient" Zintl phases. These phases represent a class of Zintl phases where the normal picture of covalent networks of singly bonded metalloids may not be sufficient to satisfy the valence requirements of the anionic substructures. Our exploratory syntheses along the Zintl border have led to the discovery of such compounds − new complex Zintl phases, $SrCa_2In_2Ge$, $Ca_5In_9Sn_6$, and Ba_2NiSi_3.[7,8] These results also emphasize the novelty of the electronic and crystal structural patterns of polar intermetallics containing trielides and tetrelides.

Earlier studies on complex Zintl phases have revealed a rich structural diversity of heteroatomic tetrahedral structures. Much of this was motivated by the desire to explore the structural chemistry of complex Zintl phases and discover a structural diversity analogous to that exhibited by complex metal oxides such as zeolites, clathrates, silicates, and aluminosilicates.[9] However, structural analogies based on an all corner-shared tetrahedral arrangement well-known in silicates and aluminosilicates have been rare among Zintl phases and related polar intermetallics. This is quite surprising since MX_4 tetrahedral units are very common in both classes of solid-state materials.

(1) (a) Nesper, R. *Prog. Solid State Chem.* **1990**, *20*, 1. (b) Nesper, R. *Angew. Chem., Int. Ed. Engl.* **1991**, *30*, 789.
(2) Novotny, H.; Reichel, H. *Powder Metall. Bull.* **1956**, *7*, 130.
(3) McNeil, M. B.; Pearson, W. B.; Bennett, L. H.; Watson, R. E. *J. Phys. C* **1973**, *6*, 1.
(4) (a) Corbett, J. D. In *Chemistry, Structure and Bonding of Zintl Phases and Ions*; Kauzlarich, S.; Ed.; VCH Publishers: New York, 1996; and references therein. (b) Pearson, W. B. *The Crystal Chemistry and Physics of Metals and Alloys*; Wiley-Interscience: New York. 1972.
(5) Belin, C.; Tillard-Charbonnel, M. *Prog. Solid State Chem.* **1993**, *22*, 59.
(6) Guloy, A. M.; Corbett, J. D. *Inorg. Chem.* **1996**, *35*, 2616.
(7) (a) Xu, Z.; Guloy, A. M. *J. Am. Chem. Soc.* **1997**, *119*, 10541. (b) Xu, Z.; Guloy, A. M. *J. Am. Chem. Soc.* **1998**, *120*, 7349.
(8) Goodey, J.; Mao, J.-G.; Guloy, A. M. *J. Am. Chem. Soc.* **2000**, *122*, 10478.
(9) Schaefer, H.; Eisenmann, B. *Rev. Inorg. Chem.* **1981**, *3*, 29.

10.1021/ic0103805 CCC: $20.00
Published on Web 07/18/2001

The few previously reported silicate and aluminosilicate analogues of Zintl phases have been limited to simple corner-shared tetrahedral chains, three-dimensional frameworks, and the unique open structures related to clathrates and zeolites.[10] However, the purported analogy to clathrates and zeolites is merely based on the tetrahedral coordination of the individual anions. Thus, the relationship between the Zintl zeolitic and clathrate Zintl phases and the metal oxide structures is restricted to individual tetrahedrally coordinated M atom (not MX_4) being analogous to a tetrahedral [SiO_4] unit. In addition, it has been mentioned that intermediate structures between tetrahedral chains and three-dimensional networks, such as "condensed ribbon and layer anions", based on the sharing of common vertexes of tetrahedral MX_4 units "are still missing" among Zintl phases.[11] Herein we describe the synthesis, crystal, and electronic structures of $Ae_2LiInGe_2$ (Ae = Ca **1**; Sr **2**), new complex Zintl phases with a layered anionic substructures composed entirely of corner-shared [$InGe_4$] tetrahedra directly analogous to the MO_4 tetrahedra in the well-known metal oxides.

Experimental Section

Synthesis. The synthesis of polar intermetallics is often associated with considerable problems. Many are attributed to the high temperatures required to induce significant reaction rates and sensitivity toward moisture, oxygen, or other adventitious impurities that complicate their handling. Furthermore, solid-state syntheses suffer from the lack of purification methods. Incidental processes such as evaporation, reactivity of containers, and adventitious impurities affect the stoichiometry of the reactions in numerous unforeseeable ways. The limited number of characterization techniques is another important facet that requires attention, and nearly all of the effective characterization methods require an adequate degree of crystallinity. Thus, the synthesis of complex Zintl phases usually incorporate the following requirements: (a) the use of high purity starting materials and clean and inert containers (e.g., Ta, Nb, Mo); (b) proper conditions for growth of crystalline products; (c) complete characterization of structure and composition, including optimizing yields.

The title compounds $Ae_2LiInGe_2$ (Ae = Ca **1**; Sr **2**) were obtained in high yields by reacting stoichiometric amounts of the pure elements (Ca pieces, 99.99%; Li ribbons, 99.9%; In shots, 99.9999%; Ge pieces, 99.9999%) in sealed tantalum ampules. The compound $Ca_2LiInGe_2$ was initially obtained from our attempts to prepare Ca_2LiIn_2Ge, which were motivated by the possibility of preparing electron-deficient Zintl phases, as in $SrCa_2In_2Ge$. The synthesis of **1** and **2** were performed under high temperatures within welded Ta tubing. The tantalum ampules, containing nominal stoichiometries of the pure elements, were welded shut under an Ar atmosphere and placed in an evacuated quartz jacket. To obtain suitable single crystals suitable for X-ray structure analysis, the tubes were heated to a temperature of 1000 °C (Ae = Sr) or 1050 °C (Ae = Ca) and held for 10 h, followed by slow cooling, over 5 days, to about 300 °C. The high-temperature reactions provided shiny silver crystals of **1** and **2** with gemlike morphology. Compounds **1** and **2** were found to be air-sensitive to the degree that powdered samples decomposed in just a few (1−3) minutes. As a general precaution, all manipulations were carried out under purified argon atmosphere in a glovebox that had a moisture level below 0.1 ppm. After proper structure characterization and chemical analysis (microprobe) was established, the compound $Ca_2LiInGe_2$ was thereafter prepared in high-yields (>95%) from reactions of stoichiometric mixtures of the pure elements. The compound $Sr_2LiInGe_2$ was directly prepared in high yields from our attempts to prepare analogues of **1**.

For physical property measurements, single-phase samples of **1** and **2** were prepared by mixing stoichiometric amounts of the constituent elements, using the prescribed synthesis procedures with a faster cooling rate. The phase composition of the samples was based on careful indexing of the X-ray powder diffraction patterns, using NBS Silicon as an internal standard. The lack of an appreciable phase width in $Ae_2LiInGe_2$ (Ae = Ca, Sr) is indicated by the evidently invariant lattice parameters ($<2\sigma$) and unit cell volumes refined from patterns of a number of nominal compositions. This is supported by the observation that single-phase samples were only obtained from reactions with nominal stoichiometry of $Ae_2LiInGe_2$. Attempts to synthesize the barium compounds have so far been unsuccessful, with BaGe and the binary indides ($BaIn_2$ and LiIn) as the predominant products.

Table 1. Crystal Data and Structure Refinement for Compounds **1** and **2**[a]

compound	**1**	**2**
empirical formula	$Ca_2LiInGe_2$	$Sr_2LiInGe_2$
formula weight	347.10	442.18
crystal system	Orthorhombic	Orthorhombic
space group	*Pnma*(#62)	*Pnma*(#62)
a/Å	7.2512(7)	7.5033(8)
b/Å	4.4380(5)	4.6194(5)
c/Å	16.902(2)	17.473(2)
volume/Å^3	543.91(10)	605.61(11)
Z	4	4
ρ (calcd)/g cm^{-3}	4.239	4.850
μ (mm^{-1})	16.894	30.906
goodness-of-fit (GOF)	1.015	1.202
R1/wR2(for observed data)	0.0187/0.0464	0.0270/0.0546
R1/wR2(for all data)	0.0201/0.0464	0.0470/0.0660
residual extremes/e Å^3	0.543, −0.767	1.239, −1.761

[a] GOF = $[\Sigma(w(F_o^2 - F_c^2)^2)/(n-p)]^{1/2}$. R1 = $(\Sigma\ ||F_o| - |F_c||)/(\Sigma\ |F_o|)$. wR2 = $[\Sigma\ w(|F_o| - |F_c|)^2/\Sigma\ w|F_o|^2]^{1/2}$.

Structure Determination. Laue photographs were used to determine the singularity of the crystals of **1** and **2**. Precession photos of **1** supported the subsequent structural refinement, indicating an orthorhombic cell in the space group *Pnma* or $Pn2_1a$. Single crystal X-ray analysis, using a Siemens SMART platform diffractometer equipped with a 1K CCD area detector, was carried out on suitably sized single crystals mounted in a glass capillary at 23 °C. The radiation used was Mo Kα monochromatized by a highly ordered graphite crystal. A hemisphere of data (1271 frames at 5 cm detector distance) was collected using a narrow-frame method with scan widths of 0.30 in ω and an exposure time of 15 s/frame (for **1**) or 40 s/frame (for **2**). The first 50 frames were remeasured at the end of data collection to monitor instrument and crystal stability, and the maximum correction on *I* was less than 1%. The data were integrated using the Siemens SAINT program,[12] with the intensities corrected for Lorentz factor, polarization, air absorption, and absorption due to variations in the path length through the detector faceplate. Empirical ψ-scan absorption corrections were applied based on the entire data sets. Redundant reflections were averaged. Final cell constants were refined using 2256 (for **1**) or 2022 (for **2**) reflections having $I > 10\sigma(I)$. The final cell constants are: a = 7.2512(7) Å, b = 4.4380(5) Å, c = 16.902(2) Å, V = 543.9(1) Å^3 for compound **1**; a = 7.5033(8) Å, b = 4.6194(5) Å, c = 17.473(2) Å, V = 605.6(1) Å^3 for compound **2**. These and other crystallographic information relevant to data collection and refinement are listed in Table 1. The Laue symmetry was determined to be *mmm*, and careful inspection of the precession photos and data set showed systematic absences consistent with $Pn2_1a$ or *Pnma*. Since the unitary structure factors displayed centric statistics, space group *Pnma* was assumed from the outset and later confirmed by subsequent crystal structure refinement. The structure was solved by direct method and refined by full-matrix least squares calculations. A solution in space group *Pnma* yielded a chemically meaningful arrangement of Ca (or Sr), In, and Ge atoms. The remaining lithium atoms were located through subsequent difference Fourier syntheses. The thermal parameters of Ca (or Sr), In, and Ge atoms were treated anisotropically and were observed

(10) Vaughey, J. T.; Corbett, J. D. *J. Am. Chem. Soc.* **1996**, *118*, 12098 and references therein.

(11) Eisenmann, B.; Cordier, G. In *Chemistry, Structure, and Bonding of Zintl Phases and Ions*; Kauzlarich, S. M. Ed.; VCH Publishers Inc: Weinheim, 1996.

(12) (a)Sheldrick, G. M. *Drogram SADABS*; Universität Göttigen, 1995. (b) Sheldrick, G. M. *SHELXTL, version 5.03*, Siemens Analytical X-ray Instruments; Madison, WI, 1995; Sheldrick, G. M. *SHELX-96 Program for Crystal Structure Determination*; 1996.

Table 2. Atomic Coordinates ($\times 10^4$) and Equivalent Isotropic Displacement Parameters ($Å^2 \times 10^3$) for Compounds **1** and **2**

atom	*x*	*y*	*z*	*U*(eq)[a]
		Compound **1**		
In(1)	8412(1)	1/4	6536(1)	18(1)
Ge(1)	2230(1)	1/4	6864(1)	16(1)
Ge(2)	7278(1)	3/4	5644(1)	16(1)
Ca(1)	8416(2)	1/4	4378(1)	19(1)
Ca(2)	5087(2)	3/4	7216(1)	17(1)
Li(1)	4865(19)	1/4	5676(7)	27(3)
		Compound **2**		
In(1)	8322(1)	1/4	6542(1)	10(1)
Ge(1)	2118(2)	1/4	6865(1)	8(1)
Ge(2)	7233(2)	3/4	5670(1)	9(1)
Sr(1)	8422(1)	1/4	4397(1)	11(1)
Sr(2)	4991(1)	3/4	7226(1)	9(1)
Li(1)	4851(29)	1/4	5665(11)	19(4)

[a] *U*(eq) is defined as one-third of the trace of the orthogonalized U_{ij} tensor.

to be well behaved. Lithium atoms in both compounds were refined isotropically. The final stages of least squares refinement showed no abnormal behaviors in the thermal and occupancy parameters, i.e., there are no mixed atomic occupancies for all the metal and metalloid sites. The final difference Fourier maps were essentially flat with the largest residual peak (0.543 $e^-/Å^3$) located less than 1 Å from Ca(1) atom in compound **1**, and a residual peak (1.239 $e^-/Å^3$) was located less than 1 Å from In(1) atom in compound **2.** Chemical analysis of several single crystals, with a JEOL 8600 electron microprobe, indicated a uniform composition and the presence of Li. Quantitative analyses resulted in the following atomic ratios: (based on In = 1.0) Ca:In:Ge = 2.018(6):1:2.036(5) for compound **1,** and Sr:In:Ge = 1.973(4):1.0:1.992(5) for compound **2**. Results of the chemical analyses are consistent with the structural refinement. Since accurate analysis for lithium based on X-rays is difficult, lithium composition was confirmed by the high yield (>95%) synthesis of the compound in reactions with ideal stoichiometry and the nearly constant lattice parameters (within 2σ) with variation of Li composition. Lattice parameters were obtained by carefully indexing powder diffraction patterns, with NBS silicon as an internal standard, with the theoretical diffraction pattern obtained from the refinement results. All calculations were made using the Siemens SHELXTL crystallographic package.[12] The atomic positions and equivalent isotropic thermal parameters of the compounds are tabulated in Table 2; the relevant interatomic distances and bond angles are presented in Table 3. Additional crystallographic data and the anisotropic displacement parameters are given in the Supporting Information. These and the F_o/F_c data are also available from A.M.G.

Physical Properties. Magnetic susceptibilities of **1** and **2** were measured using an Oxford Instruments MAGLAB 9T Vibrating Sample Magnetometer (VSM). The measurements were taken on two single-phase powder samples over the temperature range 4−300 K, at magnetic field strengths of 0.5 and 1.0 T. Each of the polycrystalline powder samples was pressed into 0.3 cm diameter pellets that were fastened to a standard sample holder with Teflon tape. All manipulations and handling of samples were performed under argon atmosphere to avoid oxidation of the air-sensitive compound. The magnetic susceptibility data were initially corrected for diamagnetic contributions from the sample holder and ion cores. Resistivity measurements were made on pressed pellets of the sample using a four-probe resistivity apparatus over the temperature range 10−300 K. For this purpose, approximately 200 mg of pressed single phase samples were prepared in an Ar atmosphere glovebox and placed in specially designed Cu sample holders for moisture sensitive materials.

Results and Discussion

Structural Description. The isomorphous compounds $Ae_2LiInGe_2$ (Ae = Ca **1**; Sr **2**) crystallize in a structure type unique to both Zintl and silicate chemistry. The crystal structure, as shown in Figure 1, can be described as having corrugated layers

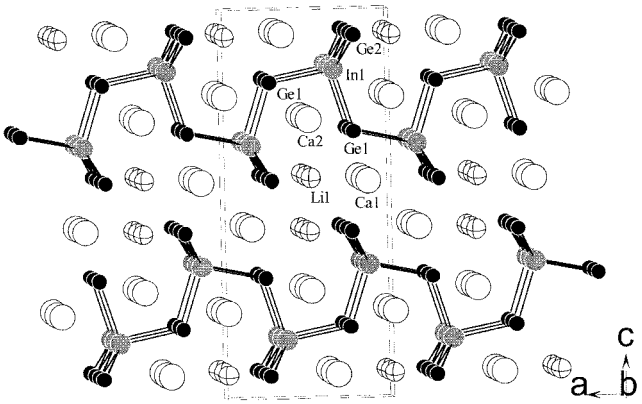

Figure 1. A [010] view of the crystal structure of $Ca_2LiInGe_2$. The Ca, Li, In, and Ge atoms are large (empty), medium (crossed), medium (gray), and small (black) spheres, respectively. The In−Ge bonds are drawn.

Table 3. Selected Bond Lengths (Å) and Angles (deg) for Compounds 1 and 2

compound		**1**	compound		**2**
In(1)−Ge(2)	2x	2.8060(6)	In(1)−Ge(2)	2x	2.8852(8)
In(1)−Ge(1)		2.8233(9)	In(1)−Ge(1)		2.904(1)
In(1)−Ge(1)		2.8377(9)	In(1)−Ge(1)		2.926(1)
Ca(1)−Ge(1)	2x	3.091(1)	Sr(1)−Ge(1)	2x	3.219(1)
Ca(1)−Ge(2)		3.122(2)	Sr(1)−Ge(2)		3.262(2)
Ca(1)−Ge(2)	2x	3.190(1)	Sr(1)−Ge(2)	2x	3.328(1)
Ca(1)−In(1)	2x	3.549(1)	Sr(1)−In(1)	2x	3.741(1)
Ca(1)−In(1)		3.647(1)	Sr(1)−In(1)		3.748(2)
Ca(2)−Ge(1)	2x	3.093(1)	Sr(2)−Ge(1)	2x	3.222(1)
Ca(2)−Ge(1)	2x	3.124(1)	Sr(2)−Ge(1)	2x	3.225(1)
Ca(2)−Ge(2)		3.096(1)	Sr(2)−Ge(2)		3.198(1)
Ca(2)−In(1)	2x	3.295(1)	Sr(2)−In(1)	2x	3.3966(9)
Ca(2)−In(1)	2x	3.473(1)	Sr(2)−In(1)	2x	3.607(1)
Ca(1)−Li(1)	2x	3.26(1)	Sr(1)−Li(1)	2x	3.37(2)
Ca(2)−Li(1)	2x	3.42(1)	Sr(2)−Li(1)	2x	3.58(1)
Li(1)−In(1)		2.95(1)	Li(1)−In(1)		3.02(2)
Li(1)−Ge(1)		2.77(1)	Li(1)−Ge(1)		2.93(2)
Li(1)−Ge(2)		2.72(1)	Li(1)−Ge(2)		2.81(2)
Li(1)−Ge(2)	2x	2.827(8)	Li(1)−Ge(2)	2x	2.92(1)
Ge(2)−In(1)−Ge(2)		104.52(3)	Ge(2)−In(1)−Ge(2)		106.36(4)
Ge(2)−In(1)−Ge(1)	2x	113.14(2)	Ge(2)−In(1)−Ge(1)	2x	112.37(3)
Ge(2)−In(1)−Ge(1)	2x	115.07(2)	Ge(2)−In(1)−Ge(1)	2x	114.51(3)
Ge(1)−In(1)−Ge(1)		96.25(2)	Ge(1)−In(1)−Ge(1)		96.75(3)
In(1)−Ge(1)−In(1)		118.92(3)	In(1)−Ge(1)−In(1)		119.20(4)
In(1)−Ge(2)−In(1)		104.52(3)	In(1)−Ge(2)−In(1)		106.36(4)

composed of corner-shared $[InGe_{4/2}]^{5-}$ tetrahedra that lie along the *ab* plane. The anionic $[InGe_2]$ layers are alternately stacked along the *c*-axis with double layers of alkaline earth and Li ions. The anionic layers can be described as being derived from nominal two-unit repeating chains (*zweierketten)*[13] of vertex-shared $InGe_4$ tetrahedra that lie along the crystallographic *a* axis. The nominal two-unit (*zweier)* chain in $Ae_2LiInGe_2$ is illustrated in Figure 2a. There are two types of germanium atoms within the *zweier* "zigzag" $[InGe_{4/2}]$ chain, namely, Ge(1) that bridges the tetrahedra along the chain axis and the terminal Ge(2). The bond distances between the central In atom to the bridging Ge(1) atoms are 2.8233(9) and 2.8377(9) Å for compound **1**, 2.904(1) and 2.926(1) Å for compound **2,** respectively, and those between the central In atom to the terminal Ge(2) are 2.8060(6) and 2.8852(8) Å, respectively, for compounds **1** and **2** (Table 3). The In−Ge−In bond angles around each bridging Ge(1) atoms are 118.92(3)° and 119.20° for compounds **1** and **2**, respectively. The two-unit *zweier* chains are found to be common building blocks of layered and three-dimensional

(13) Liebau, F. *Handbook of Geochemistry*; Springer-Verlag: Heidelberg, 1972; Vol. II/3, p 14.

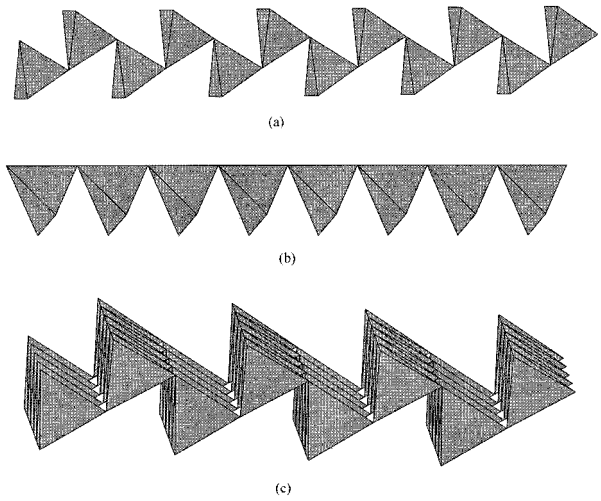

Figure 2. $InGe_4$ tetrahedra in $Ca_2LiInGe_2$. (a) The two-unit (*zweier*) chain along *a*; (b) simple one-unit (*einer*) chain along *b*; (c) the $[InGe_{4/2}]$ layer along *ab*.

silicates as in pyroxenes and cristobalite (β-SiO_2). The *zweier* chains of $InGe_{4/2}$, as described in $Ae_2LiInGe_2$, are also observed in the silicate chain structure of ht-$Ba_2Si_2O_6$.[14] Other chains of vertex-shared tetrahedra are also exhibited by complex one-dimensional anions in Zintl phases such as Sr_3GaSb_3, with a four-unit (*vierer*) chain,[15] and Sr_5SnP_3, with a simple one-unit (*einer*) chain.[16] However, further linking of these intermetallic silicate-like chains into layers of all corner-shared tetrahedra has not been previously observed in Zintl chemistry. In $Ae_2LiInGe_2$, adjacent parallel *zweier* chains are further linked by vertex-sharing of the terminal (Ge(2)) atoms along the crystallographic *b* axis. Thus, forming anionic layers of corner-shared tetrahedra, $[InGe_2]^{5-}$ The resulting $[InGe_2]^{5-}$ anionic layered structure in $Ca_2LiInGe_2$ along the *b* axis is illustrated in Figure 2c.

It is interesting to note that the anionic layer may also be described in terms of simple one-unit (*einer*) chains of corner-shared tetrahedra, $[InGe_4]$, that lie along the crystallographic *b* axis, as shown in Figure 2b. There are two crystallographic types of germanium atoms in a simple chain of vertex-shared $InGe_4$ tetrahedra, namely, a terminal (Ge(1)) and the bridging (Ge(2)). The In−Ge−In bond angles around the bridging (Ge(2)) atoms in the simple chains are 104.52(3)° and 106.36(4)°, respectively, for compounds **1** and **2**. Simple *einer* chains are commonly observed as building blocks in three-dimensional and layered structures of germanates and HgI_2, respectively.[17] Similarly, simple *einer* chains have also been observed in several one-dimensional Zintl phases containing tetrelides and pnictides. In these compounds, the simple layered structure is composed of *einer* chains connected via sharing of vertexes in a simple manner as in metallic LiSn.[17] In contrast, the simple *einer* chains in $Ae_2LiInGe_2$ (Ae = Ca, Sr) are linked via vertex sharing in a manner that generates a two-unit *zweier* arrangement along *a* axis (Figure 2c).

Within the anionic layer, all indium atoms are four-bonded to Ge and each Ge atom is bonded to two neighboring In atoms. Hence, application of the Zintl concept on the $[InGe_{4/2}]$ layer leads to a electron-precise count of: four-bonded $[In]^{1-}$ + two-bonded $2[Ge]^{2-} \rightarrow [InGe_2]$,$^{5-}$ wherein the charge of the anionic layer is compensated by two calcium and one lithium atoms per formula unit. The analogy to silicates and related nonmetal oxides in the title compounds are more accurate and direct than in any previously reported Zintl phase with zeolitic and silicate-like networks. In $Ae_2LiInGe_2$, the tetrahedrally bound In atoms are analogous with the less electronegative Si atoms, while the two-bonded Ge atoms are analogous with the more electronegative oxygen atoms of silicates, i.e., $[InGe_{4/2}]^{5-}$ is analogous and isoelectronic to $[SiO_{4/2}]$.

The crystal structure of $Ae_2LiInGe_2$ (Ae = Ca, Sr) is completed by stacking the anionic $[InGe_2]^{5-}$ layers along the *c* axis following an *a*-glide symmetry. Sandwiched between $InGe_2$ layers are double layers of alkaline earth metal (Ca or Sr) and Li atoms (Figures 1 and 3a). The alkaline earth metal (Ca1 and Sr1) atoms lie at nine coordinated sites that can be described as being formed from tetragonal pyramid of five germanium atoms (Ge1 and Ge2) and further capped by two indium and two lithium atoms (Figure 4a). The second alkaline earth metal atom (Ca2 and Sr2) occupy 11 coordinated sites (Figure 4b), which can nominally be described as a monocapped pentagonal prism (4 Ge1, + 4 In1 + 2 Li1 + Ge2). The observed Ca−Ge and Sr−Ge interatomic distances range from 3.093(1) Å to 3.124(1) Å and from 3.219(1) to 3.328(1), respectively. The observed distances are comparable to the Ca−Ge and Sr−Ge distances found in binary calcium and strontium germanides. The resulting tetrahedral coordination around Li is shown in Figure 4c. There are three different Li−Ge distances in $Ca_2LiInGe_2$ that range from 2.72(1) to 2.83(1) Å (2.81(2) to 2.93(2) Å for Sr compound), and these are comparable to those found in binary lithium germanides.[18] The corresponding Ge−Li−Ge angles are close to 109.5°, and resulting coordination of the lithium atoms is tetrahedral, each surrounded by four Ge atoms. Consequently, the alkaline earth and lithium atoms form nominal bilayers of cations sandwiched between anionic $[InGe_2]^{5-}$ tetrahedral layers.

Physical Properties. An oxidation state count, according to the Zintl scheme, for $Ae_2LiInGe_2$ indicates these air-sensitive compounds are structurally Zintl phases. The electronic and magnetic properties of $Ae_2LiInGe_2$ are consistent with this assignment. The expected semiconducting property of $Ca_2LiInGe_2$ was confirmed by four-probe resistivity measurements, which gave a resistivity at room temperature of $\rho_{298} \sim 280\ \mu\Omega$-cm, with a negative coefficient. The magnetic susceptibilities of $Ca_2LiInGe_2$ over 10−300 K were temperature independent at values of $-1.10(3) \times 10^{-4}$ emu/mol, after diamagnetic corrections for the container and ion cores. Inspection of the *M* vs *H* plots at 10 K and 300 K indicated a homogeneous diamagnetic material (no Curie "tail" was observed). The $Sr_2LiInGe_2$ compound presumably contains Sr(II) and exhibits similar semiconducting properties.

Structural Relationship with Other Tetrahedral Structures. To further understand the significance of $Ae_2LiInGe_2$, we performed a search for related crystal structures and found three related types. First is the unique β-LiSn, which features a similar structure with four-bonded and two-bonded Sn atoms

(14) Liebau, F. In *Structure and Bonding in Crystals*; O'Keefe, M., Navrotsky, A., Eds.; Academic Press: New York, 1981; Vol. II, p 197.
(15) Cordier, G.; Schaefer, H.; Stelter, M. *Z. Naturforsch* **1987**, *42b*, 1268.
(16) Eisenmann, B.; Klein, J. *Z. Naturforsch.* **1988**, *43b*, 1156.
(17) (a) Pushcharovsky, D. Y. In *Modern Perspectives in Inorganic Crystal Chemistry*; Parthé, E., Ed.; Kluwer Academic Publishers: Dordrecht, Netherlands, 1992; p 203. (b) Blase, W.; Corder, G. *Z. Kristallogr.* **1990**, *193*, 317. (c) Müller, W.; Schäfer, H. *Z. Naturforsch.* **1973**, *B28*, 246.
(18) Villars, P.; Calvert, L. D. *Pearson's Handbook of Crystallographic Data for Intermetallic Phases*; ASM International: Materials Park, OH, 1991; Vols. 1−4.

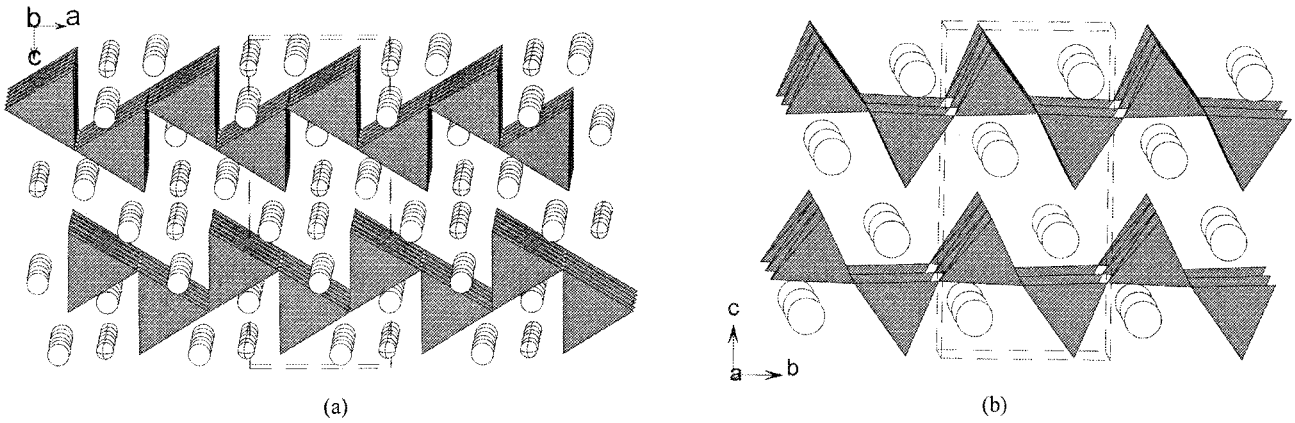

Figure 3. The tetrahedral layered structures of (a) $Ca_2LiInGe_2$, Ca: empty circles; Li: crossed circles; and (b) $SrZnO_2$, Sr: empty circles.

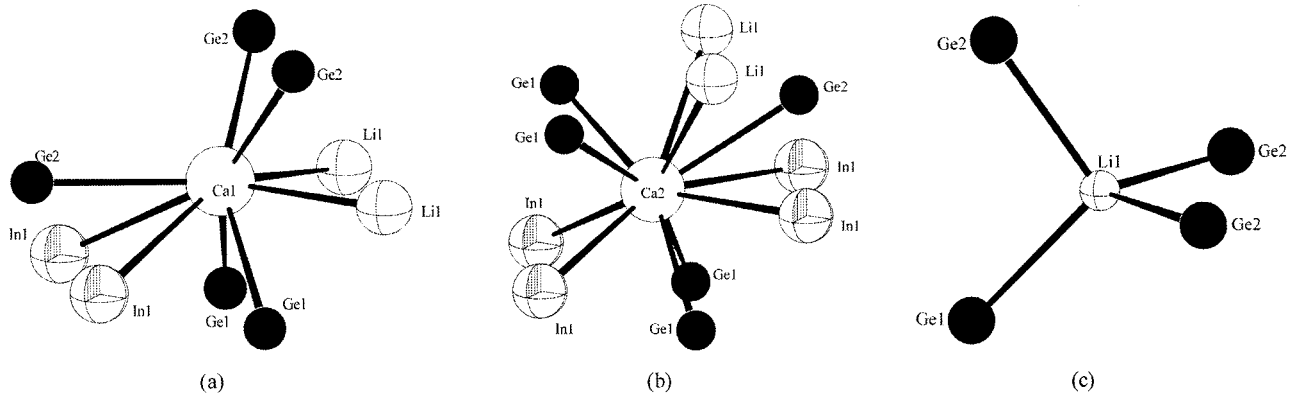

Figure 4. The coordination geometry of the cations in $Ca_2LiInGe_2$: (a) Ca(1) coordination; (b) Ca(2) coordination; and (c) Li coordination.

that form layers of *einer* chains with corner-sharing $[SnSn_4]$ tetrahedra. The "flat" $[SnSn_2]^{4-}$ sheets, separated by Li atoms, are similar to the layered HgI_2 structure. However, β-LiSn is reportedly metallic and not a Zintl phase. Moreover, tetrahedral layers composed exclusively of *einer* chains are not observed in silicate structures.[17] Second, a quaternary phase, $K_2NaInSb_2$, was reported as having a layered anionic structure, with tetrahedral $InSb_4$ units.[19] The resulting layered anion $[In_2Sb_2Sb_{4/2}]^{6-}$ is formed from the mixed corner and edge sharing of $InSb_4$ tetrahedral units—the most common linkage between tetrahedral units found in tetrahedral Zintl phases. Third, the most closely related structure to $Ae_2LiInGe_2$ is the ternary metal oxide $SrZnO_2$.[20] The layered metal oxide structure (also observed in the isostructural sulfide, $BaMnS_2$)[21] consists of $ZnO_{4/2}$ tetrahedra linked through common vertexes (Zn−O−Zn) as illustrated in Figure 3b. The $SrZnO_2$ structure features two-unit *zweier* chains, and the chains are further linked as simple *einer* links, forming a layer analogous to that observed in $Ae_2LiInGe_2$. However, the *zweier* unit in the $SrZnO_2$ structure type is "stretched" with respect to the *zweier* chains observed in $Ae_2LiInGe_2$. In addition, the "stretched" *zweier* chain in $SrZnO_2$ is structurally described as a [001] "slice" of the cristobalite β-SiO_2 structure.[20]

According to Liebau, two main parameters can be used to describe the chain units of complex silicates.[22] These are (a) the number of tetrahedra in the repeat unit, and (b) the stretching factor (ratio of the length of the repeat unit to the sum of the length of the edges of the participating tetrahedra). In complex silicates, the stretching factor mainly depends on the degree of charge transfer from the nontetrahedral countercations to the silicate anion network. To a lesser degree, the stretching factor also depends on the sizes of the nontetrahedral cations. Thus, the stretching factors of the tetrahedral chains increase with decreasing electronegativity of the nontetrahedral cations. The lower stretching factor associated with the *zweier* chains in $Ae_2LiInGe_2$ may reflect the lower polarity of the Zintl phase with respect to the metal oxides and complex silicates. Attempts to substitute larger and more electropositive cations such as barium in $Ba_2LiInGe_2$ were so far unsuccessful, resulting in the formation of BaGe and the binary barium and lithium indides. In addition, the rare structural analogy between tetrahedral Zintl phases and silicate structures can also be attributed to the restriction on the M−X−M bridging angle between tetrahedra. The bridging Si−O−Si angles in silicates that tend to be close to 140° have been rationalized in terms of the additional dπ-pπ nature of the Si−O bonds.[23] However, the In−Ge−In angles in $Ae_2LiInGe_2$ are closer to the ideal tetrahedral angle of 109.5°, as is the case in related tetrahedral chains in tetrelides and pnictides.[11] Thus, it is not surprising why polar intermetallics and Zintl phases with tetrahedral structures do not exhibit a similar structural chemistry as silicates and aluminosilicates. Nevertheless, the unique structure of $Ae_2LiInGe_2$ suggests a rich yet unique variety of tetrahedral structures, based on the vertex shared $MX_{4/2}$ tetrahedra, may exist among Zintl and polar intermetallic phases.

On the other hand, an important structural relationship between the $Ae_2LiInGe_2$ with other polar intermetallic structures

(19) Carrillo-Cabrera, W.; Caroca-Canales, N.; von Schnering, H. G. *Z. Anorg. Allg. Chem.* **1993**, *619*, 1717.
(20) von Schnering, H. G.; Hoppe, R. *Z. Anorg. Allg. Chem.* **1961**, *312*, 87.
(21) Schmitz, V. D.; Bronger, W. *Z. Anorg. Allg. Chem.* **1973**, *402*, 225.
(22) Liebau, F.; Pallas, I. *Z. Kristallogr.* **1981**, *155*, 139.
(23) Liebau, F. *Structural Chemistry of Silicates*; Springer Verlag: Berlin, 1985.

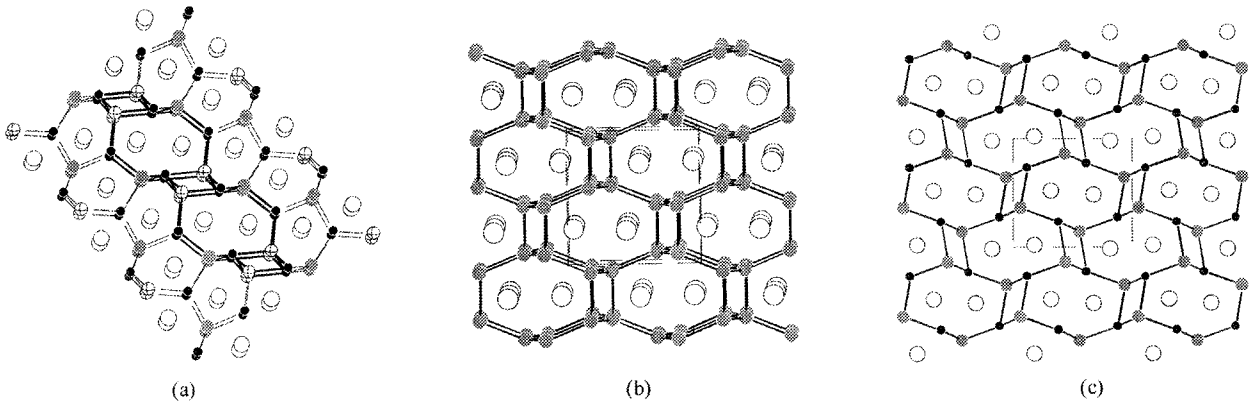

Figure 5. Crystal structures of (a) $Ca_2LiInGe_2$, the Ca, Li, In, and Ge atoms are large (empty), medium (crossed), medium (gray), and small (black) spheres, respectively; (b) $BaIn_2$, the Ba and In are empty and gray solid spheres, respectively; and (c) CaMgGe, Ca, Mg, and Ge are empty, gray, and black solid spheres, respectively. The common structural motif is outlined in (a) $Ca_2LiInGe_2$ as heavy lines.

is found when one considers the topology or connectivity of the anion network with lithium. Comparing the crystal structures of $Ae_2LiInGe_2$ with $BaIn_2$ and CaMgGe,[24] as shown in Figure 5, illustrates the relationship. Although the electron counts and structure indicate that both compounds are Zintl phases, it has been previously pointed out that the $[Mg^{2+}Ge^{4-}]$ substructure in CaMgGe can be derived from the $[In_2]^{2-}$ network of $BaIn_2$—an ordered substitution of Mg and Ge over the In sites.[24] A building unit of the $[In_2]^{2-}$ network in $BaIn_2$ is an eight-membered ring that forms tunnel-like structures filled with Ba atoms. The details of the structural differences between CaMgGe and $BaIn_2$ lie with the twisting of the $[Mg_4Ge_4]$ units in CaMgGe that can be attributed to the electrostatic repulsion between nearest neighboring Mg cations. Similarly, the $Ae_2LiInGe_2$ structure features eight-membered $[Li_2In_2Ge_4]$ rings that form a slab of parallel "tunnels" along *b* axis. The slabs are linked to adjacent slabs through In−Ge bonds forming six-membered $[LiIn_2Ge_3]$ rings. Thus, the positions of the lithium cations effectively increase the negative charge of the anion and decrease the dimensionality of the resulting anion network. This was confirmed by subsequent full three-dimensional band structure calculations on $[LiInGe_2]$.$^{4-}$ The calculations indicate a two-dimensional electronic structure associated with $[InGe_2]^{5-}$ in the title compounds.[25] The observation that small cations occupying sites in the parent anionic framework of complex polar intermetallics with large differences in cation sizes has been successfully applied to rationalize the structure of novel anion fragments with reduced dimensionality. Examples include $Ba_4Li_2Ge_6$ and $Ba_4Li_2Si_6$, wherein the $[Li_2Ge_6]$ and $[Li_2Si_6]$ layered networks represent the hexagonal layers of B_2 in the parent AlB_2 structure type.[26] The ordered arrangement of Li and Ge(Si) in the Li−Ge(Si) hexagonal networks result in the formation of novel planar hexagonal rings of $[Ge_6]^{10-}$ and $[Si_6]^{10-}$.

Concluding Remarks

We have successfully synthesized and characterized new layered Zintl phases $Ca_2LiInGe_2$ and $Sr_2LiInGe_2$ that mirror the structure of some metal oxides. The unique compounds crystallize in an unprecedented non-oxide layered structure that features corner-shared tetrahedral units, as in silicates. Thus, the syntheses of $Ae_2LiInGe_2$ (Ae = Ca, Sr) nicely illustrates a viable route in the search for new and unusual intermetallic analogues of aluminosilicates among semiconducting Zintl phases with MX_4 tetrahedral units. The title compounds portray the versatility of Zintl formalism not only in understanding but also in designing novel structures via electron count and the characteristic bonding of the constituent main-group elements.

Acknowledgment. This material is based in part on work supported by the National Science Foundation (CAREER) under award number DMR-9733587 and the Petroleum Research Fund Administered by ACS. This work made use of MRSEC/TCSUH Shared Experimental Facilities supported by the National Science Foundation under Award Number DMR-9632667 and the State of Texas through the Texas Center for Superconductivity at the University of Houston.

Supporting Information Available: X-ray crystallographic files in CIF format for the structure determination of $Ca_2LiInGe_2$ and $Sr_2LiInGe_2$. This material is available free of charge via the Internet at http://pubs.acs.org.

IC0103805

(24) (a) Nuspl, G.; Proborn, K.; Evers, J.; Landrum, G. A.; Hoffman, R. *Inorg. Chem.* **1996**, *35*, 6922. (b) Ganguli, J. K.; Guloy, A. M.; Corbett, J. D. *J. Solid State Chemistry*, **2000**, *152*, 474. (c) Eisenmann, B.; Schäfer, H.; Weiss, A. *Z. Anorg. Allg. Chem.* **1972**, *391*, 241.

(25) Xu, Z. Ph.D. Thesis, University of Houston, 1999.

(26) von Schnering, H. G.; Bolle, U.; Curda, J.; Peters, K.; Carrillo-Cabrera, W.; Somer, M.; Schultheiss, M.; Wedig, U. *Angew. Chem., Int. Ed. Engl.* **1996**, *35*, 984.